Two Dimensional Indium Selenides Compounds: An Ab-Initio Study

ARTICLE *in* JOURNAL OF PHYSICAL CHEMISTRY LETTERS · JULY 2015

Impact Factor: 7.46 · DOI: 10.1021/acs.jpclett.5b01356

1 AUTHOR:

Debbichi Lamjed

University of Lorraine

15 PUBLICATIONS **73** CITATIONS

THE JOURNAL OF PHYSICAL CHEMISTRY Letters

Letter

pubs.acs.org/JPCL

Two-Dimensional Indium Selenides Compounds: An Ab Initio Study

L. Debbichi,[†,‡] O. Eriksson,[‡] and S. Lebègue*[,†]

[†]Laboratoire de Cristallographie, Résonance Magnétique et Modélisations (CRM2, UMR CNRS 7036) Institut Jean Barriol, Université de Lorraine, BP 239, Boulevard des Aiguillettes, 54506 Vandoeuvre-lès-Nancy, France

[‡]Department of Physics and Astronomy, Uppsala University, Box 516, SE-751 20 Uppsala, Sweden

ABSTRACT: We use first-principle calculations to investigate the electronic structure of InSe and In_2Se_3. The interlayer binding energy is found to be in the same range as for other 2D systems, and the monolayers are found to be dynamically stable, which suggest the possibility to obtain them as isolated layers. The GW approximation including spin−orbit is used to obtain the bandgaps, which are in the range relevant for application in electronics. Also, it is shown that an electric field perpendicular to the layers can induce a semiconductor to metal transition in this family of compounds.

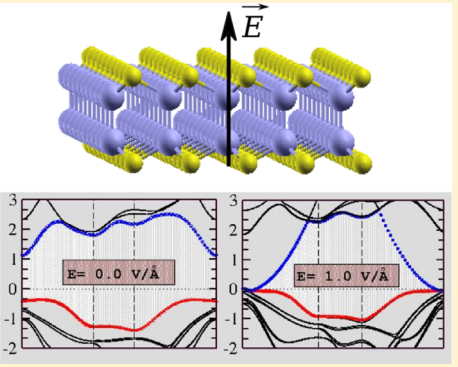

The recent successful isolation of a single or few layers of graphene[1,2] has triggered a worldwide interest in 2D materials. Graphene has shown extremely high mobilities and an impressively high breaking strength;[3,4] however, the lack of an intrinsic band gap in graphene is a major obstacle for developing field-effect-based devices and reduces its applicability in electronics. Since then, much attention has been given to search for 2D materials that can overcome the limitation of a zero band gap in graphene. Recently, various compounds have been efficiently exfoliated into individual layers with interesting structural and electronic properties. These include layers with wide bandgaps used as a complement to graphene in vertical heterostructures or for band engineering, such as h-BN,[5,6] or materials with a smaller band gap such as transition-metal dichalcogenides,[7] which form a new family of layered materials, presenting new technological properties in the ultrathin limit.[8]

However, finding materials with new properties is still desirable. Recently, layered indium selenides have also gained a renewed interest due to their properties, such as for solar energy conversion,[9] in Li-ion batteries,[10] for thermoelectricity,[11,12] and as phase-change materials for memory applications.[13] Indium selenide compounds belong to a complex family of systems with different stoichiometric ratios, including In_4Se_3, In_2Se_3, InSe, and In_3Se_4. For a given stoichiometric ratio, different phases and crystal structures may coexist, such as for In_2Se_3 (α, β,γ, δ, and κ phases) and for InSe (β and γ phases). Only the α/β-In_2Se_3 and β/γ-InSe phases are semiconducting layered structures, bonded to each other via van der Waals interactions. Recently, single and few layers of InSe[14] and α-In_2Se_3[15,16] have been synthesized via chemical and mechanical exfoliation methods and have been successfully used as photodetectors: It has been shown that both compounds are capable of having broadband photodetection from the visible to the near-infrared region with photoresponsivities superior to graphene and MoS_2.[17] Also, high-performance field-effect transistors[18] and electroluminescence[19]-based on InSe thin-films have been achieved. A strong quantum confinement effect has also been demonstrated in InSe thin films.[20] Furthermore, the $\alpha \rightarrow \beta$ phase transformation in In_2Se_3 as well as the corresponding changes in the electrical properties of thin layers have been investigated.[16] While these experimental results are quite promising, a detailed analysis of their electronic structure properties from a theoretical point of view, apart from a recent work by Zolyomi et al.,[21] focusing on a possible Lifshitz transition and on the optical properties of In_2X_2 compounds, has not been completed so far. In the present work, we investigate the binding energies and the dynamical stability of InSe- and In_2Se_3-isolated single layers. Also, the electronic bandstructures are calculated and the bandgaps are obtained with the GW approximation. Finally, the effect of the electric field on the bandstructures is studied.

Because of a difference in the stacking of the single layers, InSe exists in the β and γ polytypes belonging to the hexagonal P63/mmc and the rhombohedral $R3m$ space groups, respectively. As illustrated in Figure 1a, a single layer of InSe has a thickness of four atoms linked in the Se−In−In−Se sequence via covalent bonds with the indium atoms at tetrahedral sites. In_2Se_3 has two phases (α and β) with a layered crystallographic structure, which differ in the structure of the monolayers. The α phase (space group: $R3m$) is stable at room temperature, while the β phase (space group: $R\bar{3}m$) is stable at $T = 250$ °C.[28] Each monolayer is five atoms thick, with atoms arranged in the sequence Se−In−Se−In−Se in the direction perpendicular to the layer. The difference between the

Received: June 25, 2015
Accepted: July 18, 2015

DOI: 10.1021/acs.jpclett.5b01356
J. Phys. Chem. Lett. 2015, 6, 3098−3103

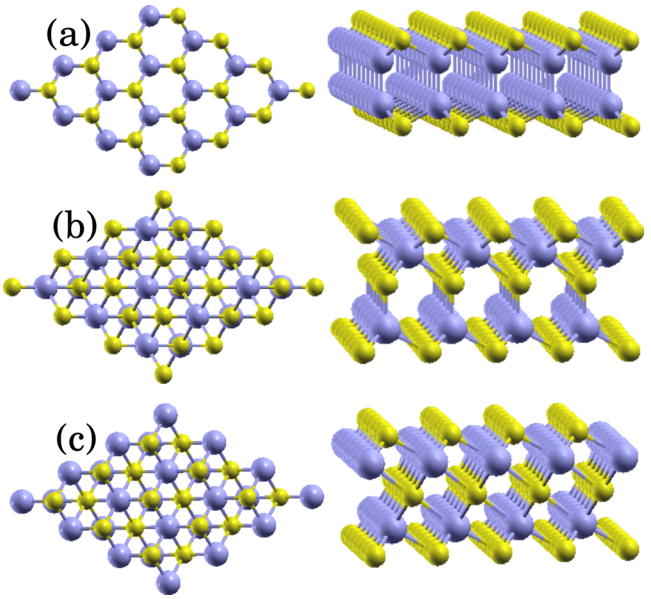

Figure 1. Top and side views of a single layer of (a) InSe, (b) In_2Se_3 (α phase), and (c) In_2Se_3 (β phase). Small (yellow) and big (blue) spheres correspond to selenium and indium atoms.

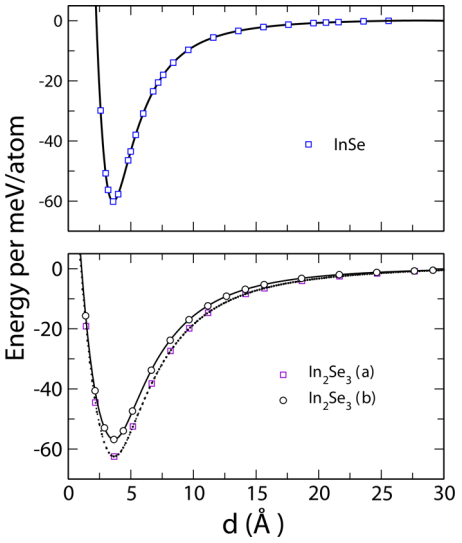

Figure 2. Calculated binding energy (meV/atom) between layers as a function of the interlayer distance (in angstroms) for InSe and In_2Se_3, as obtained with the PBE+D2 method: top is for InSe (β and γ phases, superposed) and bottom is for In_2Se_3 (α and β phases). The values obtained from our calculations are represented by spheres and squares, and the lines are a guide to the eyes.

two phases is that the indium atoms of the β phase are situated in the octahedral holes formed by the selenium atoms, while the indium atoms of the α phase are situated in tetrahedral sites[28] (see Figure 1b,c).

First, we have calculated the equilibrium lattice parameters (the crystal structures were rearranged into a hexagonal cell) and the binding energy between the layers in InSe and In_2Se_3 using Grimme's correction (see computational methods). For all of the compounds, the calculated lattice parameters are found to be in agreement with the experimental values (see Table 1), albeit with a small underestimation. The binding energies are also calculated to quantify the feasibility of the exfoliation procedure: The profile of the energy under the variation of the interlayer distance is shown in Figure 2, and the corresponding values are listed in Table 1. We found that the binding energies are practically the same for all In−Se compounds: ∼60 meV/atom. These calculated values are found to be in the same range as the estimated binding energy of graphite[32,33] (∼50 meV/atom) and of transition-metal dichalcogenides[34] (∼60 meV/atom), meaning that adjacent layers are only weakly coupled to each other. This suggests the possibility to obtain InSe and In_2Se_3 in the form of 2D isolated layers. Besides the calculation of the binding energy, we have checked the dynamical stability of each isolated single layer by calculating the corresponding phonon dispersion curve along the high-symmetry directions Γ-M-K-Γ (see Figure 3). No trace of imaginary frequencies is observed; therefore, the phonon dispersion curves suggest that the isolated 2D crystals of InSe and In_2Se_3 are dynamically stable.

As outlined above, the InSe polymorphs in the bulk form differ only by the stacking of the layers.[35] Their bandstructures (not shown here) show some similarities and correspond to a semiconductor with a direct bandgap occurring at the Γ point (for the β phase) and the Z point (for the γ phase). According to our GW calculations, the value of these bandgaps are 1.1 and 1.3 eV for the β and the γ phases, respectively. These values are in excellent agreement with the experimental data (see Table 1) and with the previous GW calculations of Ferlat et al.[36]

At the single layer limit, a direct to indirect bandgap transition is observed: Our calculated bandstructure for a single layer of InSe without spin−orbit (see Figure 4 red lines) has the minimum of the conduction bands (CBM) at the Γ point, while the valence band maximum (VBM) lies between the Γ and K points.[21] The spin−orbit coupling (SOC) induces a splitting of some bands (see black lines in Figure 4) by ∼0.12 eV, as seen, for example, at the K and M high-symmetry points. Also, the top of the valence band at Γ is slightly shifted up but without changing the nature of the gap. Our GW+SOC results are shown in Figure 4 by blue diamonds. We observe that the

Table 1. Symmetry Group, Calculated Lattice Parameters (in Å), Binding Energies (in meV/atom), and GW Bandgap E_g (Bulk and Monolayer) with Spin Orbit Coupling (in eV) of InSe and In_2Se_3[a]

	InSe		In_2Se_3	
sym	β (P63/mmc)	γ (R3mh)	α (R3mh)	β (R3$^-$mh)
a (Å)	3.95 (4.05)	3.99 (4.00)	3.93 (4.05)	4.00 (4.05[28])
c (Å)	16.92 (16.93[29])	25.31 (25.33[30])	27.9 (28.77)	29.04 (29.41[28])
E_b (meV/atom)	60	60	62	57
E_g (bulk) (eV)	1.1 (1.2)	1.3 (1.2−1.3)[10]	1.25 (1.26)[31]	0.7
E_g (ML) (eV)	2.97		1.92 (1.3)[15]	1.29

[a]Available experimental values are given in parentheses.

DOI: 10.1021/acs.jpclett.5b01356
J. Phys. Chem. Lett. 2015, 6, 3098−3103

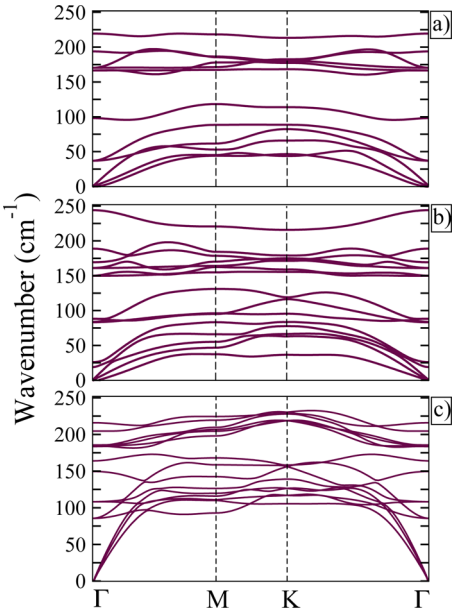

Figure 3. Calculated phonon dispersion curves of indium selenides single layers along the high-symmetry directions Γ-M-K-Γ: (a) is for InSe, (b) is for α-In_2Se_3, and (c) is for β-In_2Se_3.

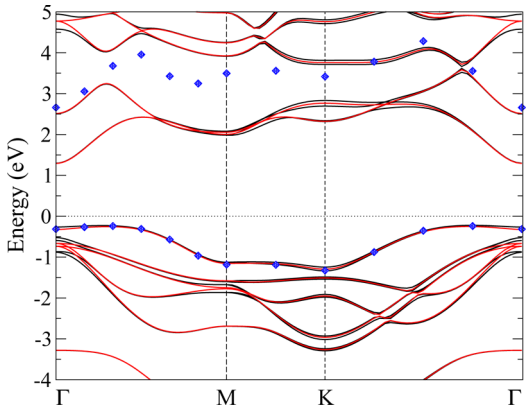

Figure 4. DFT bandstructure of a monolayer of InSe with (black lines) and without SO-coupling (red lines). The GW-SO calculations for the last valence band and the first conduction band are shown with filled diamonds. The Fermi level is set to 0 eV.

differences between PBE and GW correspond mostly to a rigid shift: there are no major quantitative differences in the dispersion of the states. (To ensure that the bandstructure remains clear, only the GW highest VB and the lowest CB calculated are shown in Figure 4.) Using PBE+SO, the bandgap is found to be 1.58 eV, but the value is increased to 2.95 eV when the GW approximation is used. Also, from the total and partial density of states (see Figure 5), the VBM is mostly dominated by p_z states from both Se and In atoms, while the bottom of the CBM is an hybridization between the Se-s, Se-p_z, and In-s states. The bandgap transition from direct to indirect was also seen by photoluminescence (PL) experiments[20] when the thickness of the layers is reduced to a few nanometers (L < 6 nm). At this thickness (corresponding to less than seven stacked layers), the optical bandgap is found to be 1.44 to 1.47 eV. A direct comparison between the experimental optical bandgap and our calculated GW electronic bandgap is difficult due to the absence of electron−hole interaction in our

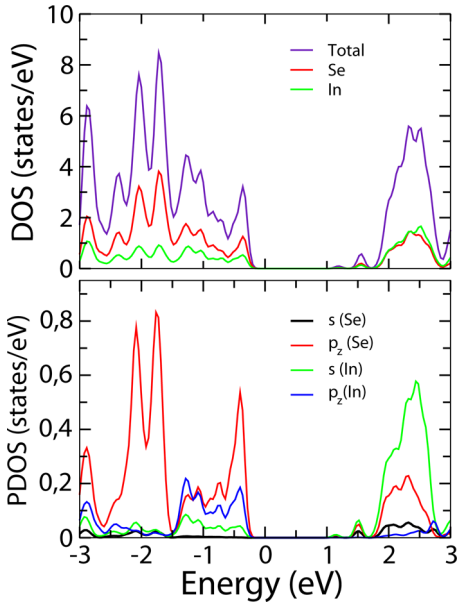

Figure 5. Calculated total and partial density of states of a single layer of InSe.

calculations. However, it was shown that in the case of transition-metal dichalcogenides, the exciton binding energies are predicted to lie in a range of 1 to 2 eV;[37] therefore, our calculated value of 2.95 eV seems realistic.

For In_2Se_3, the α and β phases in the bulk form are semiconducting with an indirect bandgap. The α phase has the VBM situated along the Γ-K direction, and the CBM is located at Γ. For β-In_2Se_3, the VBM is also found along the Γ-K direction, while the CBM is located at the M-point. With and without SO coupling, the PBE bandgap is 0.49 eV for the α phase and 0.21 eV for β phase. These calculated values are increased with the GW approximation to become 1.25 eV for the α phase, which is in excellent agreement with the available experimental data[31] and 0.7 eV for the β phase. (No experimental data were found in this case.)

At the single-layer limit, our calculated bandstructures with PBE without SO (see red lines in Figures 6 and 7) show that the α-phase and the β-phase monolayers are indirect bandgap semiconductors, with energy gaps of 0.86 and 0.54 eV, respectively; however, when the SOC is included for the α

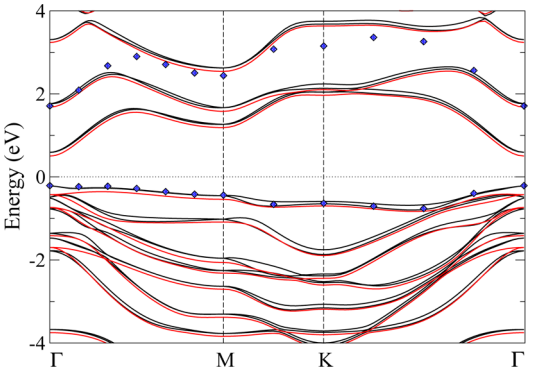

Figure 6. Calculated bandstructure of a α-In_2Se_3 single layer with (black line) and without (red line) inclusion of the spin−orbit interaction, with the filled diamonds showing the GW with spin−orbit calculation. Fermi level is set to 0 eV.

DOI: 10.1021/acs.jpclett.5b01356
J. Phys. Chem. Lett. 2015, 6, 3098−3103

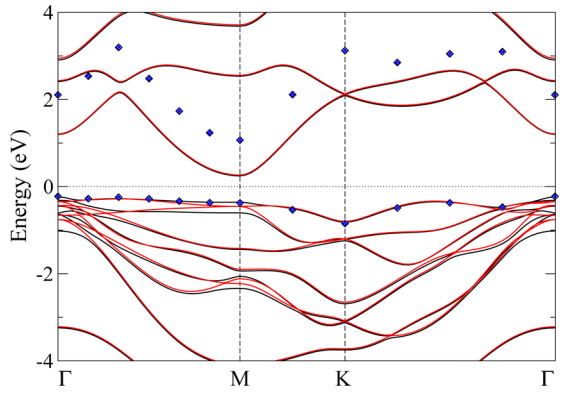

Figure 7. Calculated bandstructure of a β-In_2Se_3 single layer with (black line) and without (red line) including of the spin−orbit interaction, with the filled diamonds showing the GW with spin−orbit calculation. Fermi level is set to 0 eV.

phase (see black lines in Figure 6), the states at Γ are shifted up in energy by a few millielectronvolts and the bandgap is now direct. This finding confirms the measurement of Jacobs-Gedrim et al.,[15] in which they have obtained that 2D α-In_2Se_3 (with a ∼3.9 nm thickness) has a direct bandgap. SOC reduces slightly the bandgap to 0.82 eV with PBE+SOC, but GW+SO brings it to 1.92 eV. The effect of the SOC is also seen on the bands; for instance, a splitting of ∼0.14 eV is seen at the K point. For the β phase, the SOC does not change the nature of the bandgap as for the α phase; only the location of the VBM is changed (see Figure 7, black lines). Therefore, the β phase is an indirect semiconductor with a bandgap of 0.5 eV with PBE +SOC and of 1.29 eV with GW+SOC. As shown in the calculated partial density of states (see Figure 8), the VBM of

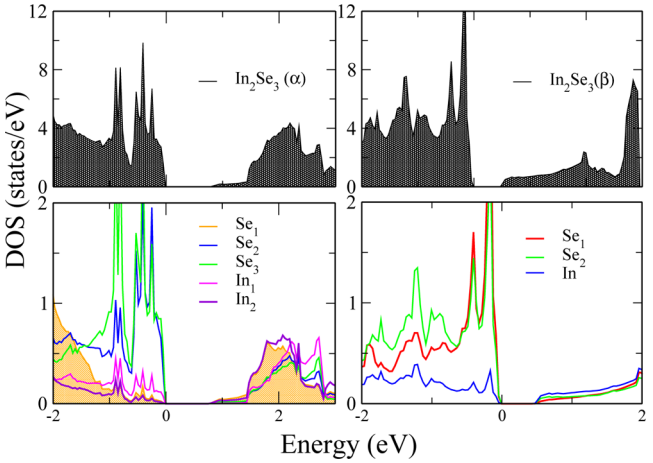

Figure 8. Calculated total and partial density of states of a single layer of In_2Se_3: The α phase is in the left panel and the β phase is in the right panel.

the α phase corresponds mainly to Se-p orbitals interacting with the In atoms in the octahedral site, while the CBM is an hybridization between the Se-p states and the In-s orbitals of the In atoms at the tetrahedral site. For the β phase, the VBM is similar to what is observed for the α phase, while the CBM corresponds to a hybridization between the Se-p and the s states of the In atoms located at the octahedral sites. Also, our calculated bandgaps for In_2Se_3 explain at least partly the origin of the different electrical resistances between the α phase and the β phase: Tao et al.[16] have shown that the resistivity is decreased by a factor of approximately two during the transition from the α to the β phase of In_2Se_3, which is consistent with the fact that we found that the α phase has a larger bandgap than the β phase.

Here we explore the effect of an external transverse electric field on the electronic structure of InSe and In_2Se_3 single layers. Indeed, the performance of electronic devices based on ultrathin layers can be controlled by applying a gate voltage,[1] which in the case of a 2D compound gives rise to an electric field perpendicular to the crystal plane.[17,38] When applying an electric field perpendicularly to a monolayer of InSe, the last occupied state is shifted up in energy at the Γ point and the dispersion of this state becomes negligible for a given region around the Γ point, resulting in an indirect to direct transition of the bandgap (see Figure 9). At the same time, a conduction band with a parabolic shape is shifted down in energy, with its lowest state in energy being ∼2 eV above the Fermi level. When the strength of the field is increased further, this band continues to be shifted down in energy, while the other bands are less affected by the electric field. Finally, for a value of ∼1.0 V/Å, the bandgap is closed, resulting in a semiconductor to metal transition for the monolayer of InSe. For the In_2Se_3 monolayers, the application of an external field is not modifying the nature of the bandgap: for the α phase, the bandgap is still direct with the VBM and the CBM located at Γ while for the β phase it is still indirect with a bandgap from the M point to the Γ point. When the magnitude of the electric field is increased to 0.5 V/Å, no significant change is observed in the bandstructure and the bangap changes slowly; however, as for InSe, a conduction band with a parabolic dispersion appears. Upon the increase in the electric field, this band is shifted down in energy and is ultimately responsible for the transition from a semiconductor to a metal, which happens around 1.0 V/Å. For the β-In_2Se_3 phase, the mechanism of the transition does not imply a band with a parabolic shape, and the transition from a semiconductor to a metal is observed at a field of only ∼0.25 V/Å due to the smaller bandgap of this phase.

Note that our calculations under electric field have been performed with density functional theory (DFT) and as shown in the previous paragraph; the value of the band gap is underestimated in this case. However, our discussion concerning the metallization still holds, although the value of electric field necessary to reach it would be higher than the one obtained from DFT. Considering the fact that our GW gaps are two to three times larger than the ones obtained with DFT, we estimate that electric fields between 2 to 3 V/Å should be sufficient to induce a insulator to metal transition in InSe and α-In_2Se_3, while a value of 0.5 V/Å should be sufficient for β-In_2Se_3. Such field strengths are available, for instance, in scanning tunnneling microscopy (STM) experiments.[39]

In conclusion, the electronic structure and the dynamical stability of InSe and In_2Se_3 single layers have been studied using DFT and the GW approximation. The calculated binding energies and phonon dispersion curves confirm the dynamical stability of these systems and the possibility to isolate them in the form of single layers. Upon the application of an electric field, we have shown than the bandgap of InSe can be switched from indirect to direct. We also predict that sufficiently strong fields induce an insulator to metal transition, a fact that may have relevance for new technology, for example, in transistor applications. We hope that our study will motivate further

DOI: 10.1021/acs.jpclett.5b01356
J. Phys. Chem. Lett. 2015, 6, 3098−3103

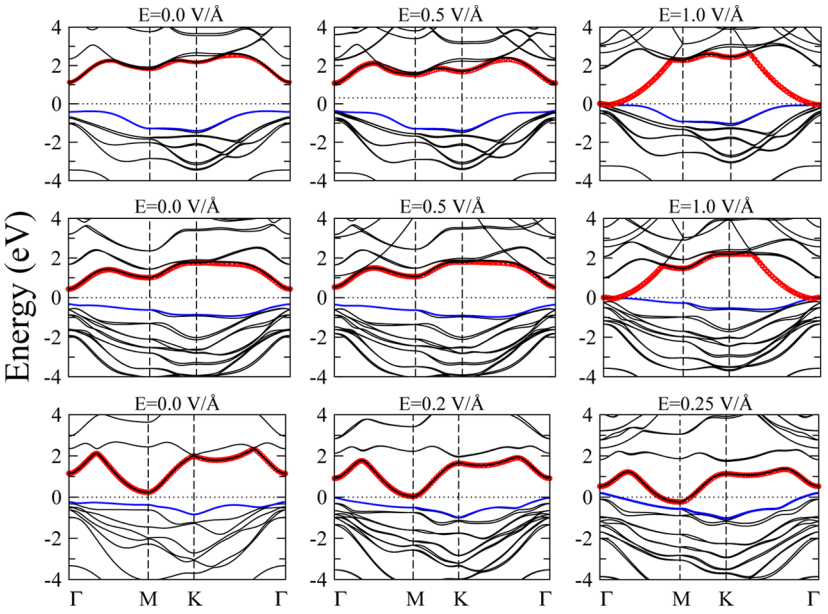

Figure 9. Evolution of the electronic band structure of InSe (top panel), α-In_2Se_3(middle panel), and β-In_2Se_3 (lower panel) single layer as a function of applied electric field. Calculations are performed with PBE and spin−orbit coupling. The top of the valence band (blue) and bottom of conduction band (red) are indicated. The Fermi level is set to 0 eV.

theoretical and experimental works on this family of 2D compounds.

The present calculations are based on DFT and the projector-augmented wave (PAW) method as implemented in the Vienna Ab Initio Simulation Package (VASP).[22] The Perdew−Burke−Ernzerhof (PBE)[23] parametrization of the generalized gradient approximation (GGA) is used for the exchange-correlation potentials with a plane wave cutoff of 400 eV and a 12 × 12 × 1 k-point mesh. Similar parameters were used for the GW calculations. van der Waals interactions were taken into account through Grimme's DFT-D2 method[24] as implemented[25] in VASP. The 2D slab geometries were set up with a vacuum space of >20 Å to ensure decoupling between periodically repeated systems. Then, each system was fully relaxed with residual forces smaller than 0.001 eV/Å. The phonon frequencies were determined using the PHONOPY code[26] for an optimized 4 × 4 × 1 supercell using density functional perturbation theory[27] (DFPT).

AUTHOR INFORMATION

Corresponding Author

*E-mail: sebastien.lebegue@univ-lorraine.fr.

Notes

The authors declare no competing financial interest.

ACKNOWLEDGMENTS

We acknowledge DARPA and Navy-NICOP for funding. O.E. gratefully acknowledges the European Research Council (ERC Project No. 247062), the Swedish Research Council (VR), SSF, and the Knut and Alice Wallenberg Foundation for financial support. O.E. also acknowledges eSSENCE and STANDUPP. This work was performed using HPC resources from GENCI-CCRT/CINES (Grant x2014-085106). Part of the calculations were performed in the Computing Centre of the Slovak Academy of Sciences using the supercomputing infrastructure acquired in project ITMS 26230120002 and 26210120002 (Slovak infrastructure for high-performance computing) supported by the Research & Development Operational Programme funded by the ERDF.

REFERENCES

(1) Novoselov, K. S.; Geim, A. K.; Morozov, S. V.; Jiang, D.; Zhang, Y.; Dubonos, S. V.; Grigorieva, I. V.; Firsov, A. A. Electric Field Effect in Atomically Thin Carbon Films. *Science* **2004**, *306*, 666−669.

(2) Meyer, J. C.; Geim, A. K.; Katsnelson, M. I.; Novoselov, K. S.; Booth, T. J.; Roth, S. The Structure of Suspended Graphene Sheets. *Nature* **2007**, *446*, 60−63.

(3) Du, X.; Skachko, I.; Barker, A.; Andrei, E. Y. Approaching Ballistic Transport in Suspended Graphene. *Nat. Nanotechnol.* **2008**, *3*, 491−495.

(4) Xia, F. N.; Mueller, T.; Lin, Y. M.; Valdes-Garcia, A.; Avouris, P. Ultrafast Graphene Photodetector. *Nat. Nanotechnol.* **2009**, *4*, 839−843.

(5) Pacilé, D.; Meyer, J. C.; Girit, ÇÖ.; Zettl, A. The Two-dimensional Phase of Boronnitride: Few-atomic-layer Sheets and Suspended Membranes. *Appl. Phys. Lett.* **2008**, *92*, 133107.

(6) Jin, C.; Lin, F.; Suenaga, K.; Iijima, S. Fabrication of a Freestanding Boron Nitride Single Layer and its Defect Assignments. *Phys. Rev. Lett.* **2009**, *102*, 195505.

(7) Novoselov, K. S.; Jiang, D.; Schedin, F.; Booth, T. J.; Khotkevich, V. V.; Morozov, S. V.; Geim, A. K. Two-Dimensional Atomic Crystals. *Proc. Natl. Acad. Sci. U. S. A.* **2005**, *102*, 10451−10453.

(8) Mak, K. F.; Lee, C.; Hone, J.; Shan, J.; Heinz, T. F. Atomically Thin MoS_2: A New Direct-Gap Semiconductor. *Phys. Rev. Lett.* **2010**, *105*, 136805.

(9) Martínez-Pastor, J.; Segura; Valdés, A.; L, J.; Chevy, A. Electrical and Photovoltaic Properties of Indium-tin-oxide/p-InSe/Au Solar Cells. *J. Appl. Phys.* **1987**, *62*, 1477.

(10) Julien, C. M.; Balkanski, M. Lithium Reactivity with III-VI Layered Compounds. *Mater. Sci. Eng., B* **2003**, *100*, 263−270.

(11) Rhyee, J.-S.; Lee, K. H.; Lee, S. M.; Cho, E.; Kim, S. I.; Lee, E.; Kwon, Y. S.; Shim, J. H.; Kotliar, G. Peierls Distortion as a Route to High Thermoelectric Performance in $In_4Se_{3-\delta}$ crystals. *Nature* **2009**, *459*, 965−968.

(12) Han, G.; Chen, Z.-G.; Drennan, J.; Zou, J. Indium Selenides: Structural Characteristics, Synthesis and Their Thermoelectric Performances. *Small* **2014**, *10*, 2747−2765.

DOI: 10.1021/acs.jpclett.5b01356
J. Phys. Chem. Lett. 2015, 6, 3098−3103

(13) Rasmussen, A. M.; Teklemichael, S. T.; Mafi, E.; Gu, Y.; McCluskey, M. D. Pressure-induced Phase Transformation of In_2Se_3. *Appl. Phys. Lett.* **2013**, *102*, 062105.
(14) Lei, S.; Ge, L.; Najmaei, S.; George, A.; Kappera, R.; Lou, J.; Chhowalla, M.; Yamaguchi, H.; Gupta, G.; Vajtai, R.; Mohite, A. D.; Ajayan, P. M. Evolution of the Electronic Band structure and Efficient Photo-detection in Atomic layers of InSe. *ACS Nano* **2014**, *8*, 1263−1272.
(15) Jacobs-Gedrim, R. B.; Shanmugam, M.; Jain, N.; Durcan, C. A.; Murphy, M. T.; Murray, T. M.; Matyi, R. J.; Moore, R. L.; Yu, B. Extraordinary Photoresponse in Two-dimensional In_2Se_3 Nanosheets. *ACS Nano* **2014**, *8*, 514−521.
(16) Tao, X.; Gu, Y. Crystalline-Crystalline Phase Transformation in Two-Dimensional In2Se3 Thin Layers. *Nano Lett.* **2013**, *13*, 3501−3505.
(17) Amalampudi, S. R.; Lu, Y. Y.; Kumar, U. R.; Sankar, R.; Liao, C. D.; Moorthy, B. K.; Cheng, C. H.; Chou, F. C.; Chen, Y. T. High Performance and Bendable Few-Layered InSe Photo-detectors with Broad Spectral Response. *Nano Lett.* **2014**, *14*, 2800−2806.
(18) Lin, M.; Wu, D.; Zhou, Y.; Huang, W.; Jiang, W.; Zheng, W.; Zhao, S.; Jin, C.; Guo, Y.; Peng, H.; et al. Controlled Growth of Atomically Thin In_2Se_3 Flakes by van der Waals Epitaxy. *J. Am. Chem. Soc.* **2013**, *135*, 13274−13277.
(19) Balakrishnan, N.; Kudrynskyi, Z. R.; Fay, M. W.; Mudd, G. W.; Svatek, S. A.; Makarovsky, O.; Kovalyuk, Z. D.; Eaves, L.; Beton, P. H.; Patanè, A. Room Temperature Electroluminescence from Mechanically Formed van der Waals III-VI Homojunctions and Heterojunctions. *Adv. Opt. Mater.* **2014**, *2*, 1064−1069.
(20) Mudd, G. W.; Svatek, S. A.; Ren, T.; Patanè, A.; Makarovsky, O.; Eaves, L.; Beton, P. H.; Kovalyuk, Z. D.; Lashkarev, G. V.; Kudrynskyi, Z. R.; et al. Tuning the Bandgap of Exfoliated InSe Nanosheets by Quantum Confinement. *Adv. Mater.* **2013**, *25*, 5714−5718.
(21) Zólyomi, V.; Drummond, N. D.; Fal'ko, V. I. Electrons and Phonons in Single layers of Hexagonal Indium Chalcogenides from *Ab initio* Aalculations. *Phys. Rev. B: Condens. Matter Mater. Phys.* **2014**, *89*, 205416.
(22) Kresse, G.; Hafner, J. Ab initio Molecular Dynamics for Liquid Metals. *Phys. Rev. B: Condens. Matter Mater. Phys.* **1993**, *47*, 558(R).
(23) Perdew, J. P.; Burke, K.; Ernzerhof, M. Generalized Gradient Approximation Made Simple. *Phys. Rev. Lett.* **1996**, *77*, 3865.
(24) Grimme, S. Semiempirical GGA-type Density Functional Constructed with a Long-range Dispersion Correction. *J. Comput. Chem.* **2006**, *27*, 1787−1799.
(25) Bučko, T.; Hafner, J.; Lebègue, S.; Ángyán, J. G. Improved Description of the Structure of Molecular and Layered Crystals: Ab Initio DFT Calculations with Van der Waals Corrections. *J. Phys. Chem. A* **2010**, *114*, 11814.
(26) Togo, A.; Oba, F.; Tanaka, I. First-principles Calculations of the Ferroelastic Transition between Rutile-type and $CaCl_2$-type SiO_2 at High Pessures. *Phys. Rev. B: Condens. Matter Mater. Phys.* **2008**, *78*, 134106.
(27) Gonze, X.; Lee, C. Dynamical Matrices, Born effective charges, Dielectric permittivity tensors, and Interatomic force constants from Density-functional Perturbation Theory. *Phys. Rev. B: Condens. Matter Mater. Phys.* **1997**, *55*, 10355.
(28) Osamura, K.; Murakami, Y.; Tomiie, Y. Crystal Structures of α- and β-Indium Selenide, In_2Se_3. *J. Phys. Soc. Jpn.* **1966**, *21*, 1848−1848.
(29) Semiletov, S. A. Electronografic Determination of the InSe Structure. *Kristallography* **1958**, *3*, 288−292.
(30) Likforman, A.; Carré, D.; Etienne, J.; Bachet, B. Structure Cristalline du Monoséléniure d'Indium InSe. *Acta Crystallogr., Sect. B: Struct. Crystallogr. Cryst. Chem.* **1975**, *31*, 1252−1254.
(31) Ye, J.; Soeda, S.; Nakamura, Y.; Nittono, O. Crystal Structures and Phase Transformation in In_2Se_3 Compound Semiconductor. *Jpn. J. Appl. Phys.* **1998**, *37*, 4264.
(32) Spanu, L.; Sorella, S.; Galli, G. Nature and Strength of Interlayer Binding in Graphite. *Phys. Rev. Lett.* **2009**, *103*, 196401.
(33) Lebègue, S.; Harl, J.; Gould, T.; Ángyán, J. G.; Kresse, G.; Dobson, J. F. Cohesive Properties and Asymptotics of the Dispersion Interaction in Graphite by the Random Phase Approximation. *Phys. Rev. Lett.* **2010**, *105*, 196401.
(34) Rydberg, H.; Dion, M.; Jacobson, N.; Schroder, E.; Hyldgaard, P.; Simak, S. I.; Langreth, D. C.; Lundqvist, B. I. Van der Waals Density Functional for Layered Structures. *Phys. Rev. Lett.* **2003**, *91*, 126402.
(35) Gomes da Costa, P.; Dandrea, R. G.; Wallis, R. F.; Balkanski, M. First-principles Study of the Electronic Structure of γ-InSe and β-InSe. *Phys. Rev. B: Condens. Matter Mater. Phys.* **1993**, *48*, 14135.
(36) Ferlat, G.; Xu, H.; Timoshevskii, V.; Blase, X. Ab initio Studies of Structural and Electronic Properties of Solid Indium Selenide under Pressure. *Phys. Rev. B: Condens. Matter Mater. Phys.* **2002**, *66*, 085210.
(37) Ramasubramaniam, A. Large Excitonic Effects in Monolayers of Molybdenum and Tungsten Dichalcogenides. *Phys. Rev. B: Condens. Matter Mater. Phys.* **2012**, *86*, 115409.
(38) Yin, Z.; Li, H.; Li, H.; Jiang, L.; Shi, Y.; Sun, Y.; Lu, G.; Zhang, Q.; Chen, X.; Zhang, H. Single-layer MoS2 Phototransistors. *ACS Nano* **2011**, *6*, 74−80.
(39) Stroscio, J. A.; Eigler, D. M. Atomic and Molecular Manipulation With the Scanning Tunneling Microscope. *Science* **1991**, *254*, 1319−1326.

DOI: 10.1021/acs.jpclett.5b01356
J. Phys. Chem. Lett. 2015, 6, 3098−3103